Neuron
Article

Directionality of Temperature Activation in Mouse TRPA1 Ion Channel Can Be Inverted by Single-Point Mutations in Ankyrin Repeat Six

Sairam Jabba,[1,5] Raman Goyal,[1,5] Jason O. Sosa-Pagán,[1] Hans Moldenhauer,[2] Jason Wu,[1] Breanna Kalmeta,[1] Michael Bandell,[3,4] Ramon Latorre,[2] Ardem Patapoutian,[3,4] and Jörg Grandl[1,*]
[1]Department of Neurobiology, Duke University Medical Center, Durham, NC 27710, USA
[2]Centro Interdisciplinario de Neurociencias de Valparaíso, Facultad de Ciencias, Universidad de Valparaíso, Valparaíso 2349400, Chile
[3]Department of Cell Biology, Dorris Neuroscience Center, The Scripps Research Institute, La Jolla, CA 92037, USA
[4]Genomics Institute of the Novartis Research Foundation, La Jolla, CA 92037, USA
[5]Co-first author
*Correspondence: grandl@neuro.duke.edu
http://dx.doi.org/10.1016/j.neuron.2014.04.016

SUMMARY

Several transient receptor potential (TRP) ion channels are activated with high sensitivity by either cold or hot temperatures. However, structures and mechanism that determine temperature directionality (cold versus heat) are not established. Here we screened 12,000 random mutant clones of the cold-activated mouse TRPA1 ion channel with a heat stimulus. We identified three single-point mutations that are individually sufficient to make mouse TRPA1 warm activated, while leaving sensitivity to chemicals unaffected. Mutant channels have high temperature sensitivity of voltage activation, specifically of channel opening, but not channel closing, which is reminiscent of other heat-activated TRP channels. All mutations are located in ankyrin repeat six, which identifies this domain as a sensitive modulator of thermal activation. We propose that a change in the coupling of temperature sensing to channel gating generates this sensitivity to warm temperatures. Our results demonstrate that minimal changes in protein sequence are sufficient to generate a wide diversity of thermal sensitivities in TRPA1.

INTRODUCTION

Somatosensory neurons detect pressure, various chemicals, and cold or hot temperatures and mediate the sensation of pain in animals. Their temperature sensitivity is enabled by expression of a set of transient receptor potential (TRP) ion channels that are activated with high sensitivity by cold or hot temperatures at various thresholds (Dhaka et al., 2006). The molecular mechanism of TRP ion channel activation by temperature is not known. TRP ion channels can be temperature activated in cell-free systems and with extremely short latency, which together is strong evidence that the composition of the membrane bilayer is not the origin of temperature sensitivity and instead the sensing mechanism is delimited to the physical state of the bilayer and the ion channel (Cao et al., 2013; Tominaga et al., 1998; Yao et al., 2009; Zakharian et al., 2010). The existence of different TRPA1 isoforms as well as studies using chimeric approaches in TRPA1 and TRPV1 demonstrate that large domains within the N terminus are involved in modulating thermal sensitivity (Cordero-Morales et al., 2011; Kang et al., 2012; Yao et al., 2011; Zhong et al., 2012). Other studies used unbiased random mutagenesis and cysteine accessibility and have pointed to the pore domain as a structure that is specifically involved in temperature activation (Grandl et al., 2008, 2010; Kim et al., 2013; Salazar et al., 2009).

An outstanding feature of TRP channels is that different members from a relatively homologous family of ion channels can have opposite thermal sensitivities, i.e., some are activated by cold temperatures, whereas others are activated by hot temperatures (Dhaka et al., 2006). Thermodynamically these differences have been well described (Baez-Nieto et al., 2011; Brauchi et al., 2004; Liu et al., 2003; Voets, 2012; Voets et al., 2004; Yao et al., 2010). However, structural correlates that determine cold sensitivity versus heat sensitivity are not firmly established (Brauchi et al., 2006). TRPA1 is arguably the most fascinating TRP ion channel in this respect, as orthologs from different species demonstrate opposite temperature directionality. For example, mouse TRPA1, human TRPA1 (80% homology with mouse), and *C. elegans* TRPA1 (22% homology) are cold activated in the presence of calcium, whereas rattlesnake TRPA1 (57% homology), rat snake TRPA1 (60% homology), and *Drosophila* TRPA1 (54% homology) are heat activated (Chatzigeorgiou et al., 2010; Cordero-Morales et al., 2011; Gracheva et al., 2010; Karashima et al., 2009; Lee et al., 2005; Sawada et al., 2007; Story et al., 2003; Tracey et al., 2003; Viswanath et al., 2003; Xiao et al., 2013; Zurborg et al., 2007).

Here, we hypothesized that specific structures (amino acid residues) mediate temperature directionality (cold versus heat sensitivity) and that mutation of these residues could perturb the temperature-activation profile. To find these residues, we performed an unbiased mutagenesis screen of a random mutant library of mouse TRPA1 (cold activated) by challenging it with hot temperatures. We identified three single-point mutations in ankyrin repeat six that are each individually sufficient to make

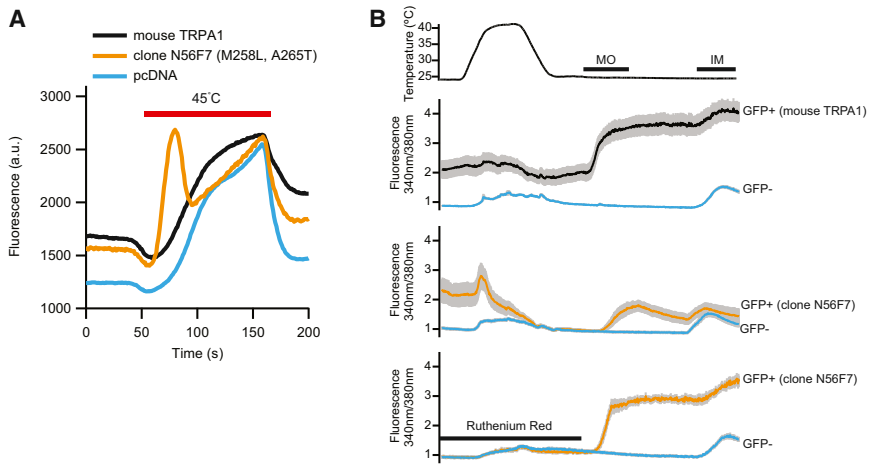

Figure 1. An Unbiased Screen Reveals Heat-Responsive Mouse TRPA1 Mutant Clones

(A) Fluorescence responses of HEK293 cells transfected with cDNA for mouse TRPA1 wild-type, pcDNA, and representative mutant clone N56F7 (plate N56, well F7) upon heating. Cells are loaded with the calcium-dye fluo-3 and measured in a FLIPR-Tetra plate reader. The mutant clone shows a transient peak response in addition to the increase seen in pcDNA or wild-type mouse TRPA1 transfected cells. Traces are averages of 4 wells (for clones) or 12 wells (for mouse TRPA1 wild-type and pcDNA).

(B) Ratiometric calcium imaging of CHO cells transfected with wild-type mouse TRPA1 or mutant clone N56F7 and exposed to a heat stimulus, 100 μM mustard oil (MO) or 1 μM ionomycin (IM), and 10 μM ruthenium red. Lines indicate averages of 30–60 cells from three different coverslips. Gray shades indicate SE.

mouse TRPA1 a warm-activated ion channel without changing sensitivity to chemical agonists. Our results suggest that temperature directionality is mediated by changes in coupling to the channel gate and that ankyrin repeat six of mouse TRPA1 is uniquely sensitive to promote this change in coupling.

RESULTS

Single-Point Mutations Are Sufficient to Make Mouse TRPA1 Warm Activated

To test our hypothesis that specific residues mediate temperature directionality (cold versus heat sensitivity), we performed an unbiased random mutagenesis screen searching for single-point mutations that could turn mouse TRPA1 (cold activated) into a heat-activated ion channel. We generated a library of 12,000 random mutant clones of mouse TRPA1 and screened it using hot temperatures (45°C) as a stimulus and measured channel activation with a calcium-influx assay (Grandl et al., 2008). We searched the library for clones that upon heat stimulation showed increased calcium levels when compared to pcDNA-transfected cells (see Experimental Procedures). From 12,000 clones, we identified and validated seven clones that show a transient but robust heat-induced calcium increase that was inhibited by the channel blocker ruthenium red (Figure 1). Sequencing of these seven clones revealed 12 point mutations. In order to find out which specific single-point mutation caused activation by hot temperatures, we then engineered all 12 mutations individually and tested heat sensitivity electrophysiologically. Since intracellular calcium can directly activate TRPA1, we performed all our electrophysiological experiments in the absence of intracellular calcium (10 mM BAPTA) (Bobkov et al., 2011; Doerner et al., 2007; Karashima et al., 2009). Chinese hamster ovary (CHO) cells transfected with cDNA coding for wild-type mouse TRPA1 or single-point mutants all showed outwardly rectifying currents when probed with a voltage-ramp protocol (±100 mV) at 25°C, whereas pcDNA-transfected cells failed to show voltage-induced currents. We then challenged patches with a temperature stimulus (25°C–40°C–25°C) and a subsequent application of 100 μM mustard oil (Figure 2A). Heating induced unspecific current increases for both inward and outward currents in all cells tested, irrespective if they were transfected with wild-type mouse TRPA1 or pcDNA control, which is likely due to a diminished seal resistance. Cells transfected with wild-type mouse TRPA1 showed a 2.8 ± 0.2-fold change in outward currents and a 3.0 ± 0.5-fold change in inward currents and cells transfected with pcDNA had a 3.6 ± 0.5-fold change in outward currents and a 2.5 ± 0.3-fold change in inward currents. Of all single-point mutants tested, three stood out because of their high heat-induced responses: S250N, M258L, and D261G. Among these three mutants, S250N evoked the highest heat response, with an average 9.8 ± 1.5-fold change in outward current (+100 mV) and 7.1 ± 1.3-fold change in inward current (−100 mV) (Figures 2B and 2C). Mutants M258L and D261G had only a modest change in outward currents, but significant increases of 6.7 ± 1.1-fold and 3.9 ± 0.7-fold in their respective inward currents. The heat-induced current increases were completely reversible in all mutants and application of mustard oil induced currents with nearly complete loss of rectification, as is typical for TRPA1. To better quantify the thermal sensitivity, we generated Arrhenius plots from representative measurements of mutant S250N, wild-type mouse TRPA1, and pcDNA-transfected cells and calculated temperature coefficients (Q_{10}) from the steep linear segments (Figure 2D). We obtained for wild-type mouse TRPA1 Q_{10} = 2.8 ± 0.3 and pcDNA Q_{10} = 1.9 ± 0.2 and for mutant S250N Q_{10} = 14.8 ± 7.9 with an activation threshold of 29.2°C ± 0.9°C. We thus identified single-point mutations that are individually sufficient to make mouse TRPA1 a warm-activated channel.

Single-Point Mutations Do Not Change Chemical Sensitivity or Channel Expression and Localization

Next, we wanted to determine the effect the identified mutations (S250N, M258L, and D261G) have on chemical sensitivity. First, we used mustard oil as a proxy for chemicals that activate TRPA1 through covalent modification of N-terminal cysteine residues (Hinman et al., 2006; Macpherson et al., 2007). We

measured concentration-response curves for all three single-point mutants in our FLIPR assay and found that responses to mustard oil were completely identical when compared with wild-type mouse TRPA1 (Figure 3A).

Caffeine is another chemical that acts on TRPA1, but it was reported to have opposite effects on different TRPA1 sequence orthologs, whereas it activates mouse TRPA1, and it inhibits human TRPA1 (Nagatomo and Kubo, 2008). In addition, this activation of mouse TRPA1 by caffeine can be inversed into an inhibition by a single-point mutation (M268P) (Nagatomo et al., 2010). Since this mutation is in close proximity to the ones we identified, we hypothesized that they might act through a common mechanism and switch the sensitivity of different agonists. We found that caffeine has a bimodal effect on wild-type mouse TRPA1 in that it causes activation at low concentrations that is diminished at higher concentrations (Figure 3B). This is reminiscent of menthol, which affects mouse TRPA1 in a similar fashion (Karashima et al., 2007; Xiao et al., 2008). To our surprise, we found that none of the single-point mutations that modify temperature sensitivity changed the effect caffeine has on wild-type mouse TRPA1 (Figure 3B).

The fact that maximal responses upon chemical stimulation were identical suggests that channel expression or more specifically the number of functional membrane-bound channels is not affected by the point mutations. To investigate this directly, we generated myc-tagged mutant channel constructs and performed immunoblots from total cell lysates (Macpherson et al., 2007). We found that total channel expression was normal for mutants S250N and D261G but slightly increased for mutant M258L as compared to wild-type mouse TRPA1 ($p > 0.05$, unpaired Student's t test) (Figure 3C). Using a biotinylation assay, we then specifically measured the membrane-bound fraction as a function of time after transfection. We found no significant differences either in the time course of protein synthesis or in the absolute amounts of biotinylated protein between wild-type mouse TRPA1 and mutant channels, indicating that overall channel stability is unchanged ($p > 0.05$, unpaired Student's t test) (Figure 3D). We further assessed channel localization by immunocytochemistry and quantified the near membrane fraction by overlap staining with wheat germ agglutinin (WGA). We found that channel membrane localization was unaffected by the mutations ($p > 0.05$, unpaired Student's t test) (Figure 3E). Altogether, these findings show that the mutations we identified do not alter either activation by chemical agonists, such as mustard oil and caffeine, or channel stability and localization.

Heat-Activated Mutations Cluster in One Ankyrin Repeat

The three mutations we identified are not scattered over the protein but are clustered in ankyrin repeat six (Figure 4A). This suggests that ankyrin repeat six plays a role in determining temperature directionality. Ankyrins consist of a conserved 33 amino acid motif that folds into one long and one short alpha helix that are connected by a short loop. A longer hairpin loop connects adjacent ankyrins and three or more units form an ankyrin repeat (Gaudet, 2008). Residue S250 is located within the predicted short loop connecting both helices, whereas residues M258 and D261 are located at the upper part of the predicted long helix (Figure 4B). These parts of the ankyrin repeats are highly conserved among different ankyrin repeat proteins and are thought to convey the general backbone structure, whereas residues within the short helix and the hairpin loop are known to give specificity to various ligands (Gaudet, 2008; Mosavi et al., 2002, 2004).

We wanted to better understand how the three mutations are located relative to each other. Since there is no crystal structure for mouse TRPA1 or its ankyrin repeats, we aligned the sequence of mouse TRPA1 with that of the ankyrin protein crystal structure that shares the highest sequence homology—the human ankyrin R (Michaely et al., 2002). The sequence homology within the helical domains of ankyrin repeat six of mouse TRPA1 and repeat 18 of human ankyrin R is very high (86% homology). Interestingly, the crystal structure of human ankyrin R reveals that residues aligning with S250, M258, and D261 all locate at the convex surface of the ankyrin repeat (Figure 4C). This common location of the three single-point mutations suggests that they mediate their effect by disrupting the native characteristic ankyrin fold rather than interfering with binding of an unknown ligand. Together, this identifies the convex surface of ankyrin repeat six as a domain that can modulate temperature directionality.

Mutation S250N Increases Temperature Dependence of Voltage Sensitivity

Voltage activates many temperature-activated TRP ion channels and voltage and temperature sensors are allosterically coupled (Brauchi et al., 2004; Latorre et al., 2007; Matta and Ahern, 2007; Voets et al., 2004). To find out how voltage sensitivity is affected, we measured whole-cell currents using voltage-step protocols at various temperatures (25°C to 40°C in 5°C increments). We focused on mutation S250N, because it demonstrated the highest temperature sensitivity. Cells transfected with pcDNA had only small voltage-activated currents at +100 mV consistent with a gigaohm seal that increased on average 1.8 ± 0.8-fold (Figure 5A). Similar to this, cells transfected with wild-type mouse TRPA1 showed an average 2.7 ± 0.5-fold increase in outward currents. This result is consistent with our data from voltage-ramp recordings. Compared to wild-type mouse, TRPA1 mutant S250N showed stronger temperature-induced increase in plateau currents (Figures 5A and 5B). However, the effect of desensitization was more pronounced, because of the relatively slow change in temperature (see Experimental Procedures). Still, the current increase from 25°C to 35°C was 4.0 ± 1.1-fold. In all patches, voltage-induced currents returned to initial levels when temperature was lowered back to 25°C (data not shown).

We then analyzed the kinetics of channel activation and inactivation upon voltage steps and found that in mutant S250N the time course of activation is strongly temperature dependent (18.3 ± 3.1 ms at 25°C versus 1.7 ± 0.4 ms at 40°C), which corresponds to a Q_{10} of 4.5 ± 1.2, whereas deactivation is nearly temperature insensitive (5.5 ± 0.8 ms at 25°C versus 3.31 ± 0.8 ms at 40°C), which corresponds to a Q_{10} = 1.5 ± 0.2 (Figure 5C). This is reminiscent of the heat-activated ion channel TRPV1, where hot temperatures specifically affect the rate of channel opening, whereas channel closing has little temperature dependence (Brauchi et al., 2004; Voets et al., 2004). Voltage

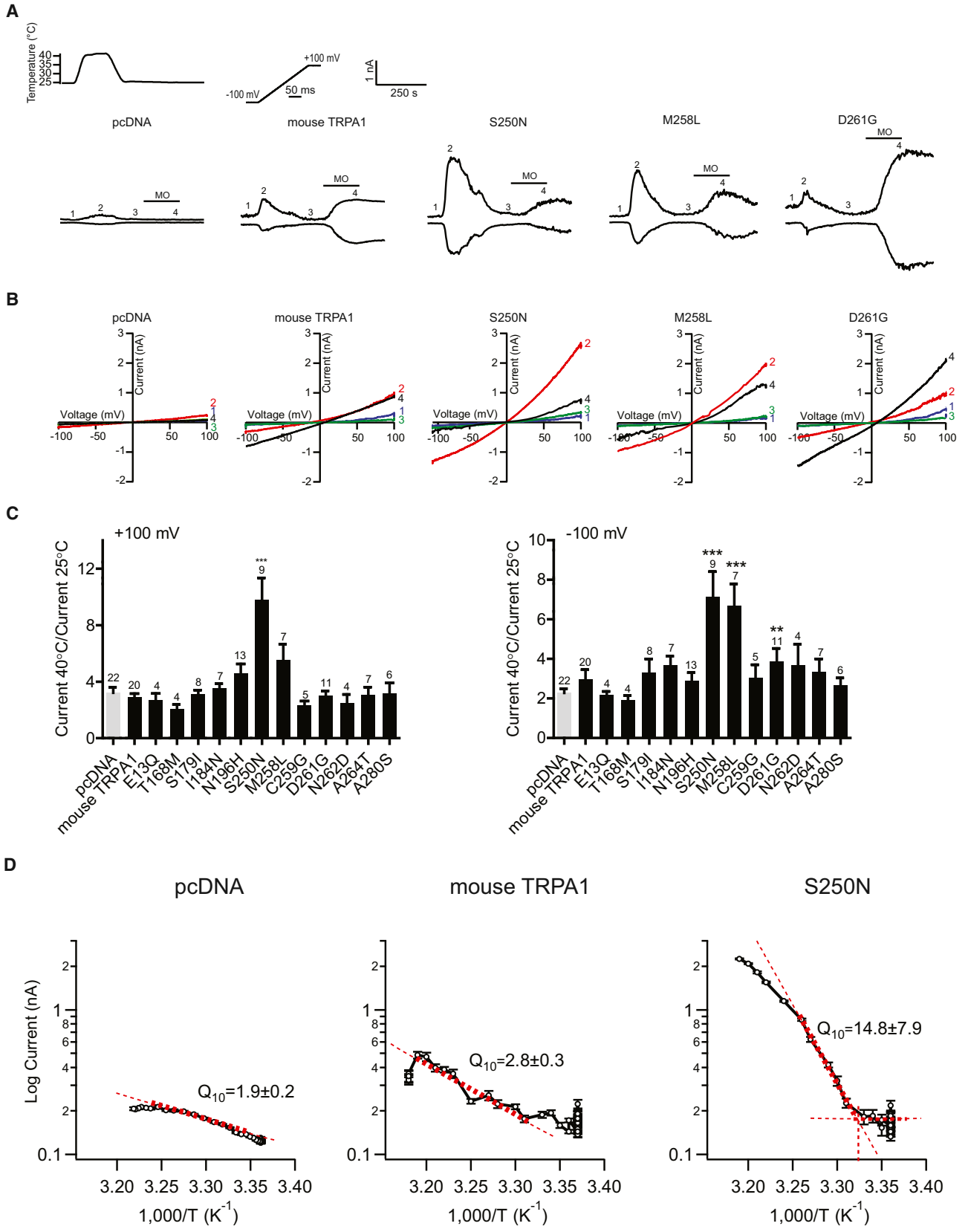

(legend on next page)

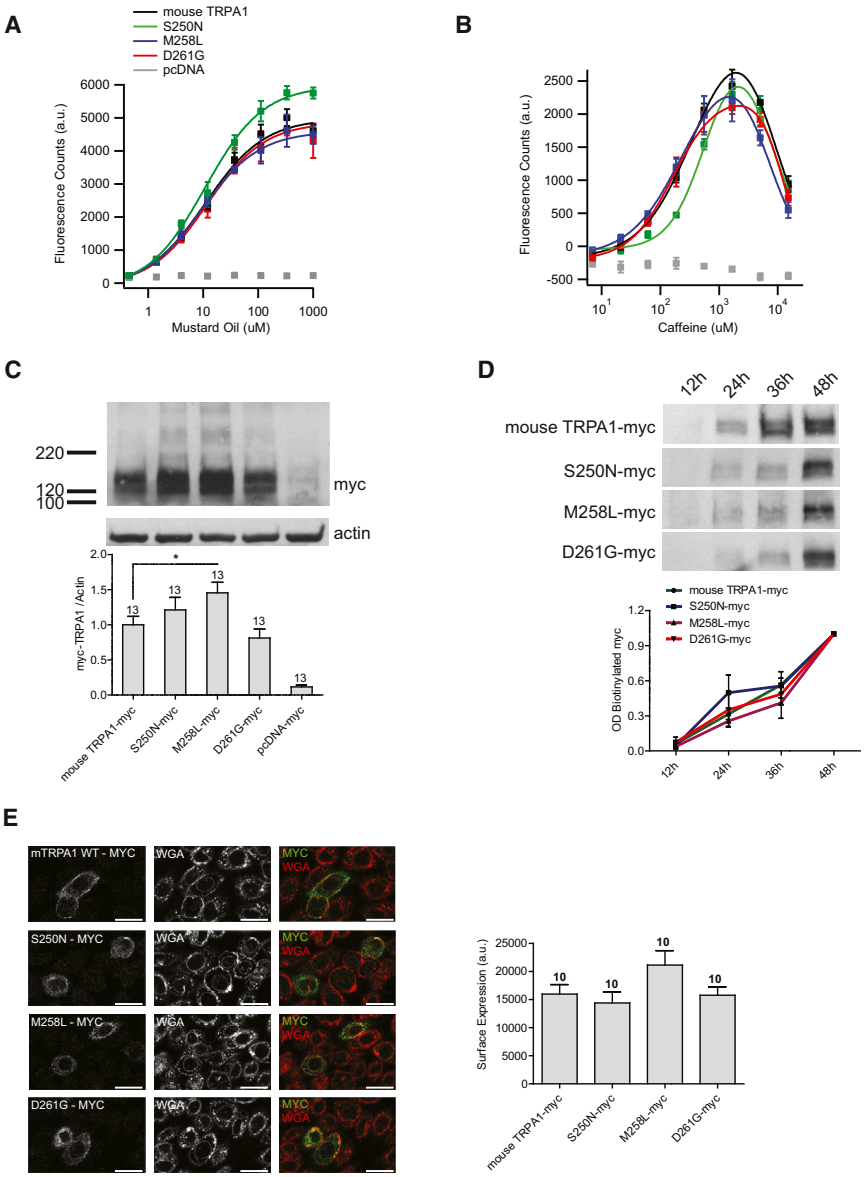

Figure 3. Effect of Single-Point Mutants on Chemical Activation, Channel Expression, and Localization

(A and B) Concentration-response curves of mustard oil (A) and caffeine (B) for heat-activated single-point mutations S250N, M258L, D261G, wild-type mouse TRPA1, and pcDNA. Data represent mean ± SD (n = 4). Straight lines indicate fits of Hill equations (mustard oil) or double-Hill equations (caffeine). For mustard oil, S250N EC_{50} = 10.8 ± 1.5 μM; M258L EC_{50} = 9.4 ± 2 μM; D261G EC_{50} = 11.7 ± 2.7 μM; and wild-type mouse TRPA1 EC_{50} = 11.1 ± 1.6 μM. For caffeine, S250N EC_{50} = 0.6 ± 0.4 mM, IC_{50} = 7.2 ± 6.3 mM; M258L EC_{50} = 0.3 ± 0.3 mM, IC_{50} = 6.7 ± 3.3 mM; D261G EC_{50} = 0.2 ± 0.1 mM, IC_{50} = 11.9 ± 1.5 mM; and wild-type mouse TRPA1 EC_{50} = 0.4 ± 0.1 mM, IC_{50} = 8.2 ± 0.1 mM.

(C) Western blots of whole-cells lysates obtained from CHO cells expressing mouse TRPA1-myc, S250N-myc, M258L-myc, and D261G-myc. Bar graph represents band intensity normalized to actin. Data represent mean ± SE, n = 13.

(D) Representative immunoblots of biotinlyated surface protein elutes obtained from CHO cells transfected with wild-type mouse TRPA1-myc or S250N-myc, M258L-myc or D261G-myc 12 hr, 24 hr, 36 hr, and 48 hr after transfection. Graph represents band intensity at different time points normalized to the amounts at 48 hr. Each data point is an average of at least three measurements. Data represent mean ± SE.

(E) Representative confocal images of cells expressing myc-tagged channel constructs stained with myc (green) and WGA (red). Graph shows quantification of near-surface levels of myc-tagged channel constructs. Data represent mean ± SE, n = 10 cells.

itself had no significant effect on the time constants of activation and deactivation (data not shown). These data demonstrate in more detail that mutation S250N generates strong heat sensitivity in mouse TRPA1.

We calculated conductance-voltage (G-V) curves from the plateau currents of these recordings and determined the voltage of half-maximal activation (V_{half}) (Figure 5D). We found that for S250N mutant channels, the V_{half} at 25°C was higher (67.0 ± 7.6 mV) than for wild-type mouse TRPA1 (45.1 ± 6.0 mV) (Figure 5D). In addition, we observed that for mutant S250N heating strongly shifted the V_{half} to more negative potentials (67.0 ± 7.6 mV at 25°C to 27.8 ± 7.8 mV at 40°C, $p < 0.05$, unpaired Student's t test), whereas in wild-type mouse TRPA1 heating did not affect the V_{half} significantly (45.1 ± 6.0 mV at 25°C to 41.2 ± 3.2 mV at 40°C, $p > 0.05$, unpaired Student's t test). We therefore conclude that mutation S250N induces a

Figure 2. Warm Temperatures Activate TRPA1 Single-Point Mutants

(A) Whole-cell recordings of transiently transfected CHO cells in Ca^{2+}-free buffer. Representative currents evoked by ramp protocol (±100 mV) for pcDNA, wild-type mouse TRPA1, and mutants S250N, M258L, and D261G during a temperature step, followed by application of MO (100 μM). Numbers indicate basal currents (1), peak responses (2), recovery currents (3), and mustard oil application (4).

(B) Current-voltage relationships at indicated time points.

(C) Average of maximal current amplitudes at ±100 mV for different single-point mutants. Numbers of experiments are indicated above bars. Data represent mean ± SE. Stars indicate statistical significance as compared to pcDNA (***$p < 0.001$, **$p < 0.01$).

(D) Representative Arrhenius plots at ±100 mV. Data represent mean ± SD. Dotted lines indicate weighted exponential fits to sections before and after channel activation. n = 9 for mutant S250N, n = 16 for wild-type mouse TRPA1, and n = 4 for pcDNA.

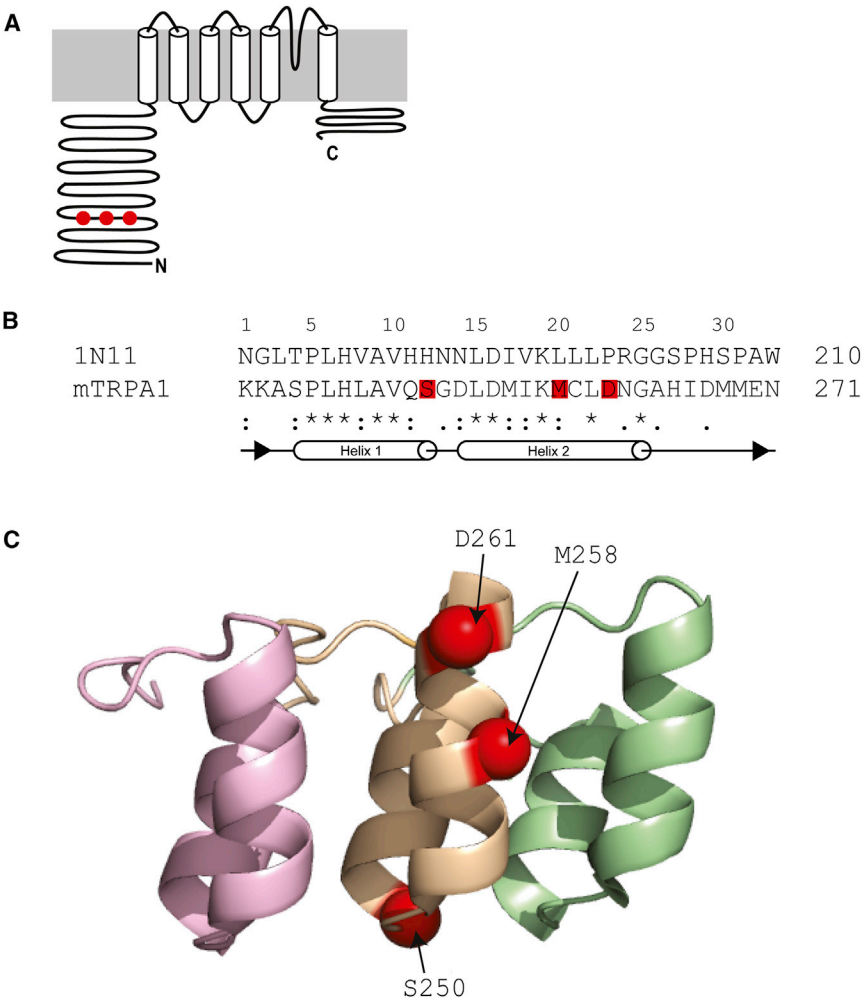

Figure 4. Location of Single-Point Mutations

(A) Topology of TRPA1 with locations of identified single-point mutations indicated in red.

(B) Sequence alignment of ankyrin repeat six of wild-type mouse TRPA1 and ankyrin repeat 18 of human ankyrin R generated with ClustalW. "*" indicates identical amino acids and ":" and "." similar amino acids. Identified point mutations are highlighted in red. Secondary structures are indicated below.

(C) Structure of repeats 17–19 of human ankyrin R (1N11). Residues corresponding to mouse TRPA1 S250, M258, and D261 are highlighted as red balls.

strong temperature dependence on the voltage sensitivity, which is again reminiscent of other temperature-activated TRP channels (Brauchi et al., 2004; Voets et al., 2004). Altogether, these findings show that mutation S250N specifically generates temperature activation and temperature sensitivity of voltage activation, without affecting activation by chemical agonists.

Mutation S250N Reduces Cold Sensitivity of Wild-Type Mouse TRPA1

It had been reported before that in the absence of calcium wild-type mouse TRPA1 is a mildly cold-activated ion channel (Chen et al., 2013; Karashima et al., 2009; Sawada et al., 2007). We probed the effect of cold temperature (13°C) on wild-type mouse TRPA1 using whole-cell recordings and a voltage-step protocol (−140 mV to +100 mV) in calcium-free conditions. To overcome desensitization, we built a rapid solution-switching perfusion enabling temperature changes (25°C to 13°C) within less than 10 s (see Experimental Procedures). We found that in wild-type mouse TRPA1 cooling increases voltage-induced currents in a reversible manner (Figure 6A). The effect was small (40.4% ± 9.8% increase at +100 mV) but consistent across all patches tested. On the contrary, currents in cells transfected with pcDNA were consistently reduced (48.7% ± 5.6% reduction at +100 mV) upon cooling. Therefore, our results support that in the absence of calcium mouse TRPA1 is mildly cold activated. Next, we wanted to know if the cold activation of wild-type mouse TRPA1 was preserved in mutant S250N. Here, we found that cold temperatures also increased plateau currents (15.2% ± 13.9% increase at +100 mV). However, the change was reduced in comparison to wild-type mouse TRPA1, suggesting that mutation S250N makes the channel less sensitive to cold.

The temperature dependence of voltage gating is arguably a better measure of temperature sensitivity, because it is not skewed by desensitization. We therefore calculated G-V curves from these recordings (Figure 6C). We found that in wild-type mouse TRPA1 cooling shifted the V_{half} toward more negative potentials from 48.2 ± 1.4 mV at 25°C to 41.2 ± 2.4 mV at 13°C ($p < 0.05$, unpaired Student's t test). This temperature dependence of voltage sensitivity is characteristic of temperature-activated TRP channels and further substantiates that in the absence of calcium wild-type mouse TRPA1 is a mildly cold-sensitive ion channel. On the contrary, in mutant S250N, cold temperatures shifted the voltage of half-maximal activation to more positive potentials, although the change was small and statistically not significant (57.0 ± 4.2 mV at 25°C to 61.2 ± 5.4 mV at 13°C, $p > 0.05$, unpaired Student's t test). This further supports the idea that mutation S250N diminishes the weak sensitivity of wild-type mouse TRPA1 to cold temperatures.

Calcium is known to potentiate the cold sensitivity of wild-type mouse TRPA1 (Karashima et al., 2009). We therefore repeated the previous experiment in the presence of 2 mM extracellular calcium (Figure 6C). We found that in wild-type mouse TRPA1 cooling induced a strong current increase (531% ± 213% at +100 mV) that was absent in cells transfected with pcDNA (26% ± 12% decrease) and nearly abolished in mutant S250N (40% ± 23% increase). Altogether, these experiments show that mutation S250N strongly reduces or completely abolishes the sensitivity to cold temperatures.

Mutation S250N Increases Temperature Dependence of Open Probability, but Not Unitary Conductance

High temperature sensitivity can originate from either temperature sensitivity of the unitary conductance *i* or the open probability P_o or both. High temperature dependence of the unitary conductance would be an indication of conformational changes of the pore itself. In fact, pore dilation and changes in ion selectivity have been described in TRPA1 and other TRP ion channels (Banke et al., 2010; Chen et al., 2009; Chung et al., 2005, 2008). On the contrary, high temperature dependence of the open probability would point toward an effect on channel gating. To measure the temperature dependence of unitary conductance, we recorded single-channel activity in the cell-attached configuration with a voltage-step protocol (±120 mV) at various temperatures (5°C to 40°C) (Figure 7A). For each temperature, we measured the single-channel current at various potentials and calculated the unitary conductance from linear fits. At 25°C, the unitary conductance of wild-type mouse TRPA1 at positive potentials was 122 ± 9 pS. The unitary conductance of mutant S250N was similar to wild-type mouse TRPA1 (124 ± 14 pS). In addition, we found that for both channels the unitary conductance at positive potentials had identical temperature dependence in mouse TRPA1 (Q_{10} = 1.4 ± 0.1) and in the S250N mutant (Q_{10} = 1.4 ± 0.1) (Figure 7B). This degree of temperature dependence is expected from the diffusion of ions in aqueous solution and is therefore not indicative of structural effects of heat on the pore itself.

Next, to determine the effect mutation S250N has on open probability, we continuously recorded single-channel activity in the inside-out configuration (+100 mV) upon temperature stimulation (Figure 7C). Similar to cell-attached recordings, we saw occasional single-channel openings in both wild-type mouse TRPA1 and mutant S250N at 25°C. In contrast, single-channel events were nearly completely absent from all control patches of pcDNA-transfected cells, indicating that the observed activity originated from wild-type or mutant TRPA1 channels. We further observed that a heat stimulus (25°C–40°C–25°C) strongly increased single-channel activity in patches with mutant S250N, whereas hot temperatures caused no change in channel activity in patches with wild-type mouse TRPA1. To quantify this observation, we calculated the change in open probability ($N \cdot P_o$). The results confirmed that heating increased the open probability in mutant S250N (12.8 ± 8.9-fold), but not in wild-type mouse TRPA1 (0.8 ± 0.4-fold). Taken together, the temperature dependences of unitary conductance and open probability are consistent with that of total currents measured in our whole-cell experiments. These data demonstrate that mutation S250N renders TRPA1 heat activated, specifically because of inducing strong heat sensitivity in open probability but not unitary conductance.

Point Mutations and Replacement of Ankyrin Repeat 6 in *Drosophila* TRPA1

The sequence homology of ankyrin repeat 6 between mouse TRPA1 and the heat-activated rat snake TRPA1 is very high (>61%) (Figure 8A). Specifically, the three residues we identified in our screen are conserved (S250 and M258) or identical (D261 and E261, both acidic). However, in the heat-activated *Drosophila* TRPA1, all three residues are different compared to mouse TRPA1 (Figure 8A). This comparison demonstrates that these three residues cannot be exclusively sufficient to determine temperature directionality among TRPA1 orthologs and suggests that additional structures (domains) are required.

To test the possibility that the entire ankyrin repeat 6 constitutes a domain that is sufficient in setting temperature directionality, we generated chimeric channel constructs by swapping ankyrin repeat 6. Mouse TRPA1 with ankyrin repeat 6 of *Drosophila* TRPA1 (mTRPA1-dmAR6) and *Drosophila* TRPA1 with ankyrin repeat of mouse TRPA1 (dmTRPA1-mAR6) did not respond to heat or cold or mustard oil, suggesting that overall channel function was lost and that despite high sequence homology, ankyrin repeat 6 is not generally interchangeable (Figure S1).

How would the single-point mutations we identified in mouse TRPA1 affect temperature sensitivity in *Drosophila* TRPA1? We individually mutated the two aligning residues G276N and K287G of *Drosophila* TRPA1 (L284 is identical) and tested their sensitivity to cold and hot temperatures. We found that in *Drosophila* TRPA1 mutation G276N completely ablated channel responses to hot temperatures without inducing sensitivity to cold temperatures (Figure S1 and data not shown). Contrary to this, heat responses remained unchanged in *Drosophila* TRPA1 K287G as compared to wild-type *Drosophila* TRPA1 (Figures 8B–8D). Specifically, the temperature sensitivity (Q_{10} = 10.9 ± 3.7 for wild-type *Drosophila* TRPA1 and Q_{10} = 19.6 ± 5.7 for *Drosophila* TRPA1 K287G, $p > 0.05$, unpaired Student's t test) and temperature threshold (30.7°C ± 1.0°C for wild-type *Drosophila* TRPA1 and 32.7°C ± 1.4°C for *Drosophila* TRPA1 K287G, $p > 0.05$, unpaired Student's t test) remained unchanged. Together, these data demonstrate that temperature sensitivity in *Drosophila* TRPA1 is not perturbed by mutations in ankyrin repeat 6 in an identical manner.

DISCUSSION

We set out to identify structures that determine the directionality of temperature activation in TRP ion channels, i.e., activation by cold versus hot temperatures. We followed the rationale that such structures when perturbed by mutations could switch temperature directionality. We discovered by using an unbiased random mutagenesis screen and patch-clamp electrophysiology three single-point mutations that are each individually sufficient to make mouse TRPA1 heat activated. The point mutation with the strongest temperature phenotype S250N generates a heat receptor with a high temperature sensitivity (Q_{10} = 14.8 ± 7.9). Although this temperature dependence is lower than that of other temperature-sensitive TRP channels (e.g., TRPV1 Q_{10} ~26 and TRPM8 Q_{10} ~24) (Brauchi et al., 2004; Liu et al., 2003; Voets et al., 2004), it is comparable to that of other TRPA1 orthologs (e.g., rattlesnake Q_{10} = 13.9, rat snake Q_{10} = 8.8) (Cordero-Morales et al., 2011; Gracheva et al., 2010).

TRP ion channels are distinct in that they are activated by many physically diverse stimuli, and these activation mechanisms are allosterically connected (Brauchi et al., 2004; Latorre et al., 2007; Voets et al., 2004). Yet, it had been shown that distinct activation mechanisms can be functionally separated

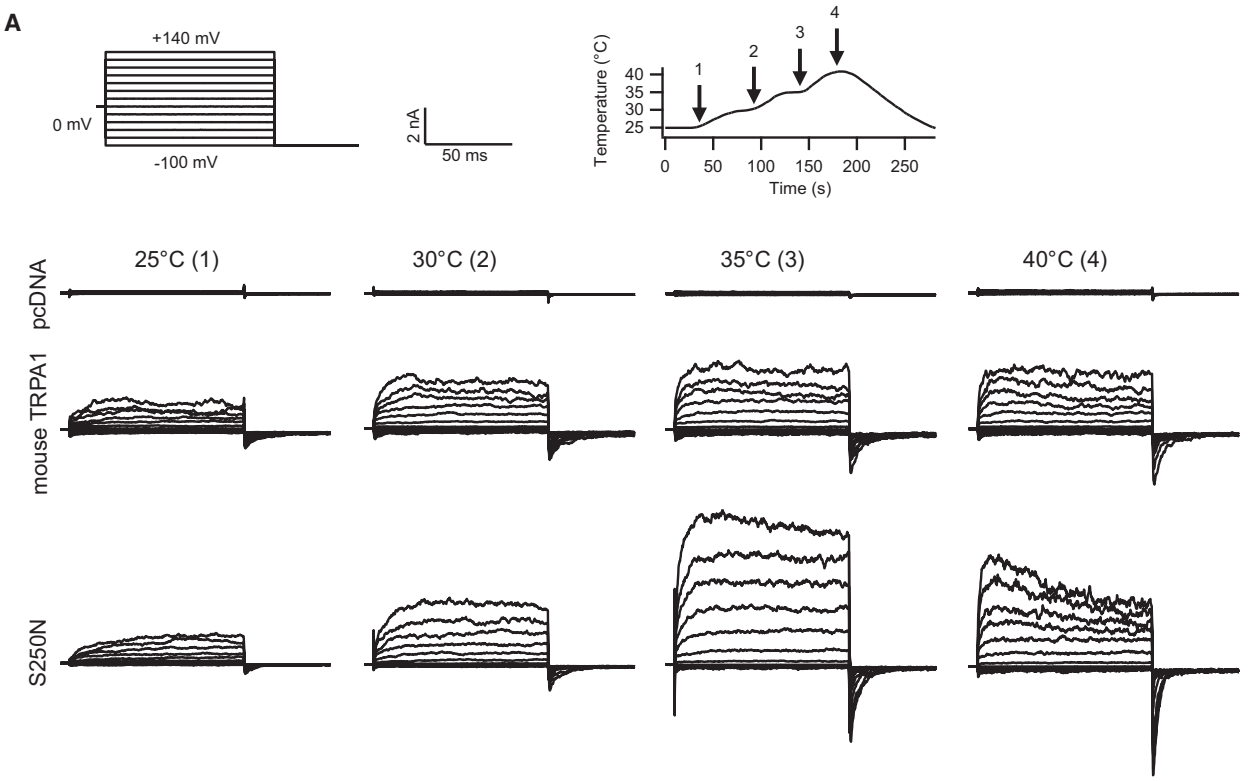

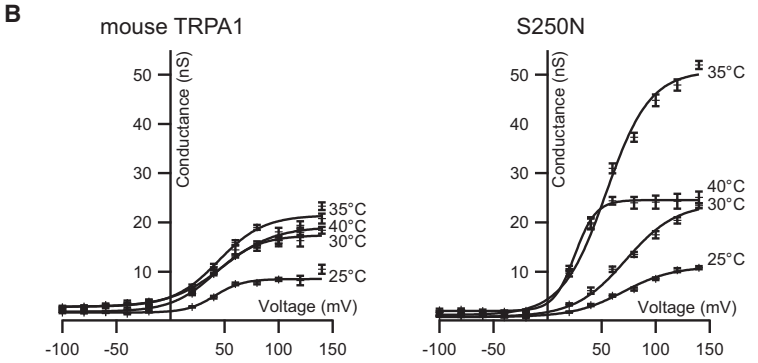

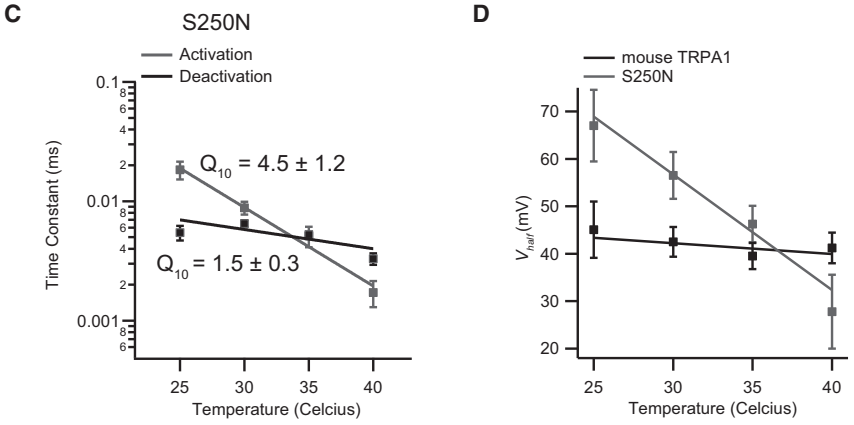

(legend on next page)

in TRPV3, TRPV1, and TRPM8, either by mutations that selectively ablate one activation mechanism or by combined application of saturating stimuli (Bandell et al., 2006; Grandl et al., 2008, 2010; Hu et al., 2009; Jordt and Julius, 2002; Jordt et al., 2000; Matta and Ahern, 2007). Although we did not select our clones for chemical responsiveness, the mutations we identified here are stimulus specific in that they have a profound effect on temperature sensitivity and temperature dependence of voltage sensitivity, but not chemical sensitivity. The data therefore highlight that TRPA1 has, like other polymodal TRP ion channels, distinct modular functionalities.

We were interested in how the existence of a single-point mutation that turns TRPA1 into a heat-activated ion channel could be explained mechanistically. At least three distinct concepts for temperature activation have been put forward.

First, temperature sensitivity has been explained by a mechanism that is based on a fine balance of large changes in enthalpy and entropy (Brauchi et al., 2004; Liu et al., 2003; Voets et al., 2004). Within this mechanism, changes in enthalpy (ΔH) and entropy (ΔS) upon gating have to be large but must have the opposite sign in cold-sensitive and heat-sensitive channels. For example, in heat-activated TRPV1 ΔH ~+150 kcal/mol, whereas in cold-activated TRPM8 ΔH ~−110 kcal/mol (Brauchi et al., 2004; Liu et al., 2003; Voets et al., 2004). This is important, because this large energy difference between a heat-activated and a cold-activated ion channel cannot be generated by a single amino acid substitution, unless this mutation produces structural changes on a large scale. In other words, a single amino acid is unlikely to contain an independent thermosensitive domain.

A second alternative mechanism for temperature activation was proposed, where temperature gating is not based on large changes in enthalpy and entropy but instead driven by changes in heat capacity (Clapham and Miller, 2011). As a consequence, TRP channels are predicted to be activated by both hot and cold temperatures (and closed at intermediate temperatures). Another important prediction of the heat capacity mechanism is that thermal sensitivity (Q_{10}) is equal for both cold and hot temperatures. As is the case with all native TRP channels, we do not see any strong sign of this dual sensitivity in our mutants. Also, voltage sensitivity is predicted to have a nonlinear temperature dependence. We observed perfect linearity in our S250N mutant within 25°C and 40°C, where the channel was heat activated, but not within 25°C and 13°C. However, this experimentally accessible temperature window is too narrow to firmly establish a deviation from linear temperature sensitivity. Moreover, 40–80 residues are estimated to be required for a sufficiently large change in heat capacity (Clapham and Miller, 2011). Following the same energetic argument as above, it is unlikely that a single amino acid substitution induces a change in heat capacity of this order of magnitude. Rather, the phenotype we identified could be best explained by mutations shifting the temperature of minimal channel activity.

Third, very recently it had been directly proposed that temperature directionality could be determined by the degree of allosteric coupling of a unidirectional temperature sensor to the channel gate, instead of assuming the existence of separate cold sensors or heat sensors (Jara-Oseguera and Islas, 2013). Applied to our data, this would mean that each of the three point mutations alters the coupling of the sensor to the gate to such a degree that a switch of temperature directionality becomes apparent.

Clearly, although these three proposed mechanisms of temperature activation differ substantially in nature, they all agree in that the phenotype we discovered could be best explained by a substantial change in the coupling of temperature sensing to channel gating and not by altering the nature (directionality) of the sensor itself. This conclusion is important, because other studies have addressed the question of modular temperature domains before. One study found that the C-terminal domains of TRPV1 (heat activated) and TRPM8 (cold activated) can confer temperature directionality (Brauchi et al., 2006). Other studies have pointed to the N-terminal domain as a modulator of thermal sensitivity: two large domains, each consisting of six ankyrin repeats (~200 amino acids) in the heat-activated rattlesnake TRPA1 are sufficient to confer heat sensitivity to the temperature-insensitive human TRPA1 ortholog (Cordero-Morales et al., 2011). Similarly, splice variants of *Drosophila* TRPA1 that differ in a 37 amino acid domain within the N terminus have distinct temperature sensitivities (Kang et al., 2012; Zhong et al., 2012). Identically, the N-terminal linker region (76 amino acids) between the ankyrin repeats and the first transmembrane domain can confer thermal sensitivity of rat TRPV1 to human TRPV2 (Yao et al., 2011). In mouse TRPA1, cold sensitivity can be abolished by a single amino-acid change (Chen et al., 2013). Our study differs from all of the above studies in that we found that a gain in temperature sensitivity can be achieved by single-point mutations versus replacement of large domains. This argues that similar to the interpretation we have for our data, swapping of larger domains between different TRP channels or addition of domains in splice variants could change channel gating instead of transporting a temperature-sensing domain.

Interestingly, all three heat-activated mutations we discovered are not scattered all across the protein but are localized in ankyrin repeat six of the N-terminal domain. How do the

Figure 5. Effect of Hot Temperature on Gating of Wild-Type Mouse TRPA1 and Mutant S250N

(A) Representative whole-cell recordings upon voltage steps (−100 mV to +140 mV) in Ca^{2+}-free intracellular and extracellular solutions at consecutive temperatures steps of 5°C.

(B) Representative conductance-voltage (G-V) curves of plateau currents at different temperatures. Data represent mean ± SD. Lines indicate fits of a Boltzman function to the data.

(C) Activation and deactivation rates of mutant S250N at +140 mV as a function of temperature. Data represent mean ± SD. Lines indicate exponential fits to the data

(D) Voltage of half-maximal activation ($V_{1/2}$) as a function of temperature. All above data represent mean ± SE, n = 4 for wild-type mouse TRPA1, n = 5 for mutant S250N, and n = 4 for pcDNA. Straight lines indicate linear fits to the data.

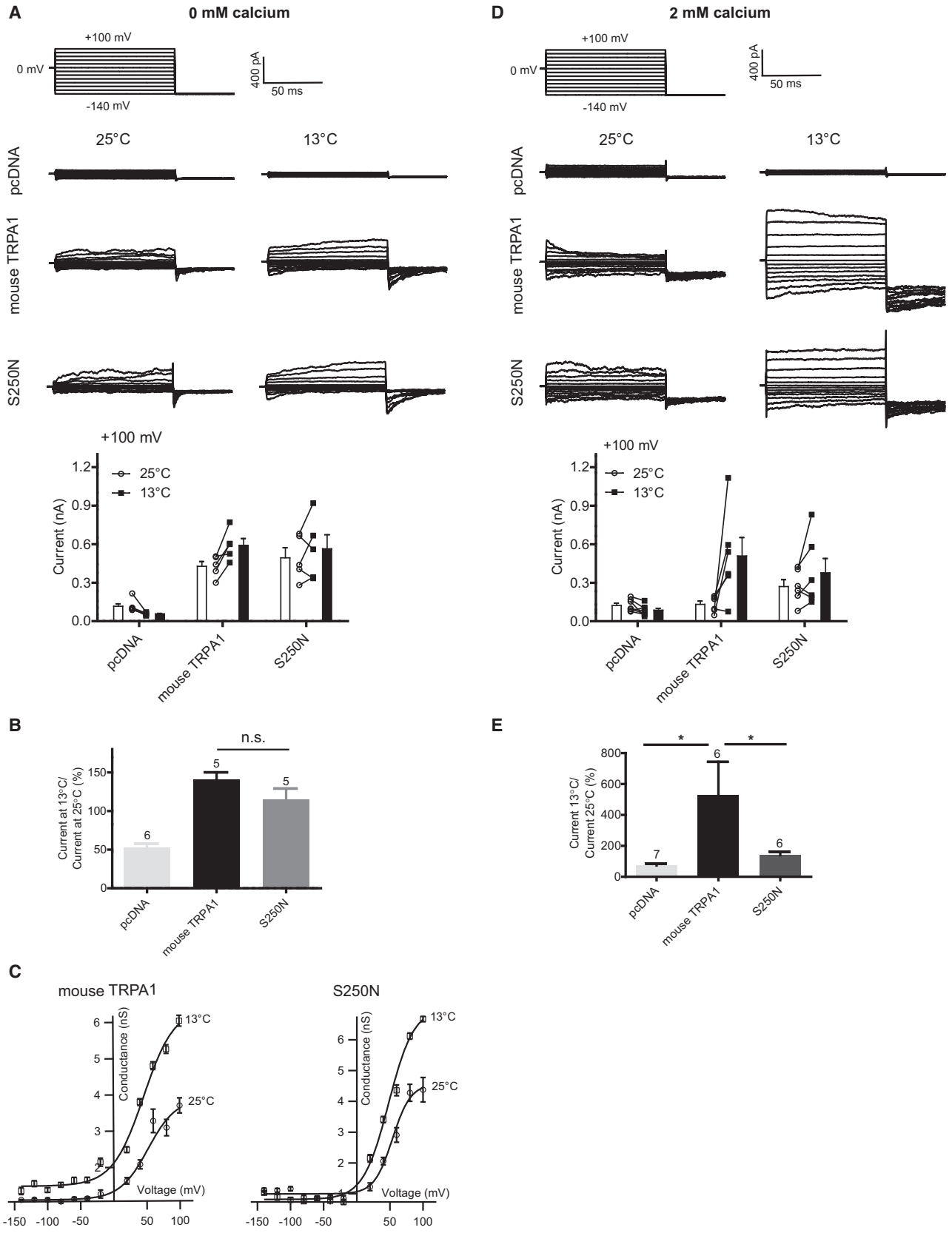

(legend on next page)

structures identified in other studies (C-terminal domain, ankyrin repeats, N-terminal linker) relate to this? All of the above domains had been identified by the same approach of constructing chimeric proteins (Brauchi et al., 2006; Cordero-Morales et al., 2011; Kang et al., 2012; Yao et al., 2011; Zhong et al., 2012). Our study was different in that it was unbiased, i.e., the entire protein was uniformly tested, and in that we screened for the effect of comparably small structural changes, i.e., single residues versus large coherent domains. By default, our screen was therefore unlikely to discover all domains that can affect the gating of temperature activation but was instead biased to find structures that are most sensitive to mutations. Our study therefore highlights ankyrin repeat six as a sensitive structure that when mutated can modulate temperature gating. Interestingly, the recent high-resolution structure of the heat-activated TRPV1 revealed that one of its six ankyrin repeats interacts with a β sheet structure within the C terminus of the adjacent subunit (Liao et al., 2013). It is unclear whether a similar interaction exists within TRPA1 orthologs, but it is obvious how mutations within an ankyrin repeat could interfere with this coupling and affect channel gating. Collectively, our data demonstrate that minimal changes in the protein sequence of a TRP ion channel can cause opposite temperature sensitivities. This functional plasticity might have been a key to evolve a single ancestor ion channel into the wide diversity of temperature-activated ion channels we know today.

EXPERIMENTAL PROCEDURES

Mutant Library Generation

A library of 12,000 random mutant clones of mouse TRPA1 was generated by using the GeneMorph II Random Mutagenesis Kit (Strategene). Specifically, from wild-type mouse TRPA1 in a pcDNA3.1(−) we separately mutagenized an N-terminal fragment (~1,800 bp) and a C-terminal fragment (~1,500 bp), separated by a unique Cla1 restriction site. For several test reactions, 20 randomly selected clones were fully sequenced to adjust PCR conditions to an average mutation rate of 12 ± 2/10,000, which corresponds to approximately two amino acid changes per fragment. Subsequently, the respective mutagenized PCR fragments were ligated into wild-type mouse TRPA1 vector and transformed into XL-10 Gold competent cells. We selected 12,000 clones and prepared miniprep DNA as described before (Bandell et al., 2006).

Site-Directed Mutagenesis and Chimeras

Single-point mutations were generated using the QuikChange Site-Directed Mutagenesis Kit (Agilent) and fully sequence verified. Chimeras of mouse and *Drosophila* TRPA1 were constructed using overlapping PCR (Agilent) and fully sequence verified.

Cell Culture

CHO cells were cultured in Ham's F-12K Media (Life Technologies) with 10% heat-inactivated fetal bovine serum (Life Technologies), 50 units/ml penicillin, and 50 mg/ml streptomycin (Life Technologies). Cells were harvested by incubating with 0.05% trypsin (Sigma). Cells were transiently transfected by adding suspended cells to a mix of DNA, Fugene, and Opti-MEM according to manufacturer's protocol (Promega). For 384-well assays, cells were seeded at 400,000/ml (25 μl/well). For electrophysiology, cells were seeded in the presence of 10 μM ruthenium red at 25,000/ml (1 ml/well) on 10 mm glass coverslips (Warner Instruments). Cells were incubated at 37°C and 5% CO_2 for 16–72 hr prior to experiments.

Library Screening and Mutant Selection

We washed 384-well assay plates with HANKS buffer, loaded them with fluo-3, and washed them with HANKS buffer as described before (Grandl et al., 2008). The mutant library was screened on a FLIPR Tetra (Molecular Devices): 384-well assay plates were heated from 25°C to 45°C for 120 s each using a custom-made device (Grandl et al., 2008). For each individual plate, the background signal from pcDNA-transfected cells (n = 4) was subtracted and clones were selected if they showed an increased signal over pcDNA upon heat stimulation in three or four wells. From the primary screen, 108 clones were selected and fresh minipreps prepared and rescreened in an identical assay on two separate plates. From this experiment, 25 clones were confirmed and further selected. Clones were regrown and Maxi-prep DNA prepared for a third screen on one single plate from which seven clones were confirmed and selected.

Calcium Imaging

Cells plated on glass coverslips were loaded with pluronic acid containing 2 μM Fura-2 AM (Invitrogen) and dissolved in HANKS buffer (Sigma) at room temperature for 30–60 min. Cells were imaged every second with an inverted microscope (Nikon) at 340 nm and 380 nm. Movies were analyzed with Nikon Elements software: background was subtracted, regions of interest for GFP-positive and GFP-negative cells selected, and the 340/380 ratio calculated.

Immunoblotting

Total lysates from CHO cells transfected with myc-tagged TRPA1 and mutant plasmids were prepared in ice-cold RIPA lysis buffer with freshly added protease inhibitor cocktail, PMSF, and sodium orthovanadate (Santa Cruz Biotechnology), scraped, sonicated, and cleared by centrifugation. We added 2× Laemmli Sample Buffer (Bio-Rad) containing 50 mM DTT (Sigma) to total lysates and heated it to 37°C for 30 min. Denatured samples were subjected to SDS/PAGE and western blotting (anti-myc antibody, Invitrogen). Signal intensity was measured by ImageJ (NIH).

Surface Biotinylation

Transfected CHO cells were washed three times with ice-cold PBS and incubated in PBS containing 0.5 mg/ml Sulfo-NHS-SS-biotin (ProteoChem) for 30 min. The biotinylation reaction was quenched in PBS containing 50 mM glycine by washing three times for 5 min each. Cell lysates were collected and cleared as described. Cleared lysates were incubated with NeutrAvidin

Figure 6. Effect of Cold Temperature on Wild-Type Mouse TRPA1 and Mutant S250N

(A) Representative whole-cell recordings of wild-type mouse TRPA1, pcDNA, and mutant S250N upon voltage steps (−140 mV to +100 mV) in Ca^{2+}-free intracellular and extracellular solutions at 25°C and 13°C (n = 5). Line plots indicate individual experiments and adjacent bars represent the average current of all recordings at 25°C (open) and 13°C (closed).

(B) Bar graph represents relative change in plateau currents upon cooling (25°C–13°C) in wild-type mouse TRPA1, pcDNA, and heat-activated mutant S250N at +100 mV. Numbers of experiments are indicated above bars. Data represent mean ± SE.

(C) Representative conductance-voltage (G-V) curves of plateau currents of wild-type mouse TRPA1 and heat-activated mutant S250N at 25°C and 13°C. Numbers of experiments are indicated above bars. Data represent mean ± SD. Lines indicate fits of a Boltzman function to the data.

(D) Representative whole-cell recordings of wild-type mouse TRPA1, pcDNA, and mutant S250N upon voltage steps (−140 mV to +100 mV) in 2 mM calcium extracellular solution at 25°C and 13°C. Line plots indicate individual experiments and adjacent bars represent the average current of all recordings at 25°C (open) and 13°C (closed).

(E) Bar graph represents relative change in plateau currents upon cooling (25°C–13°C) in wild-type mouse TRPA1, pcDNA, and heat-activated mutant S250N at +100 mV. Numbers of experiments are indicated above bars. Data represent mean ± SE.

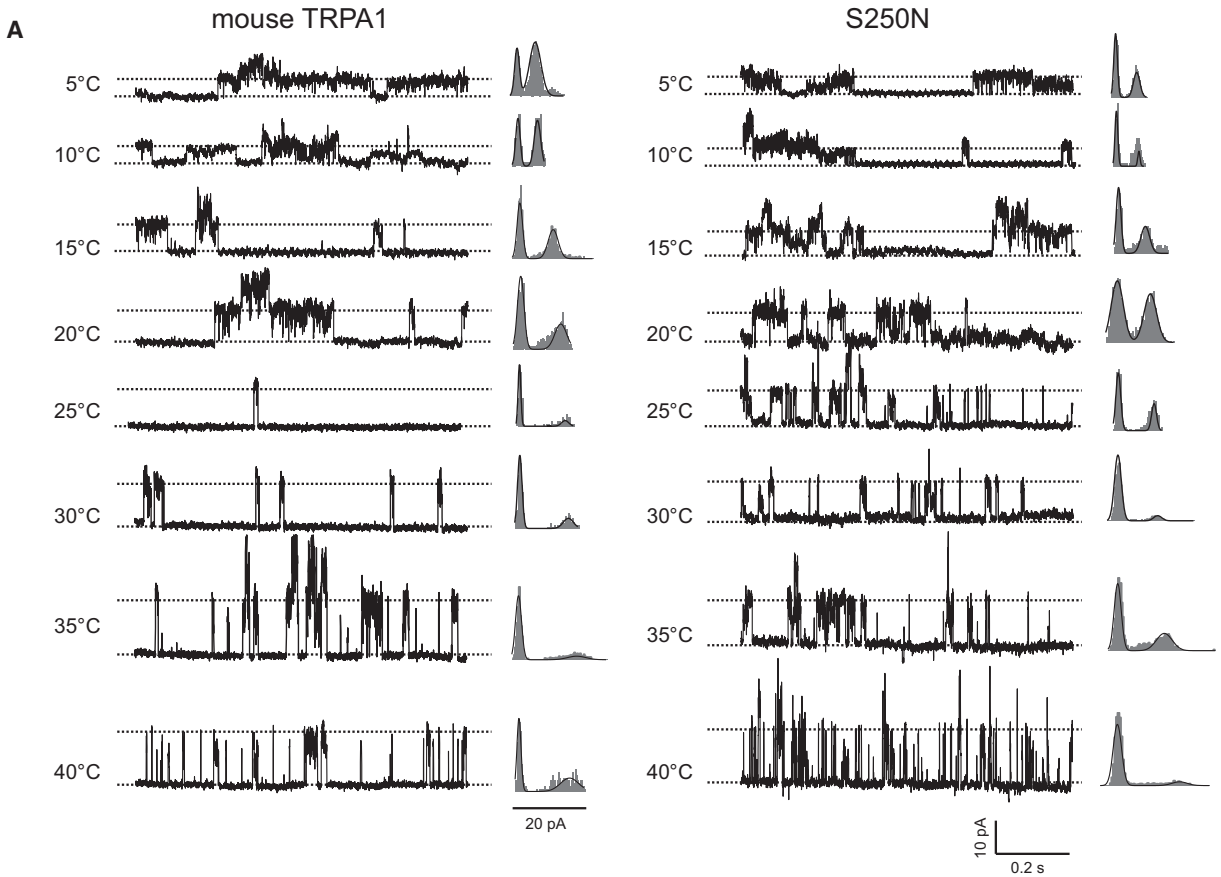

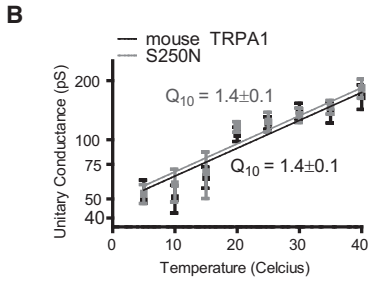

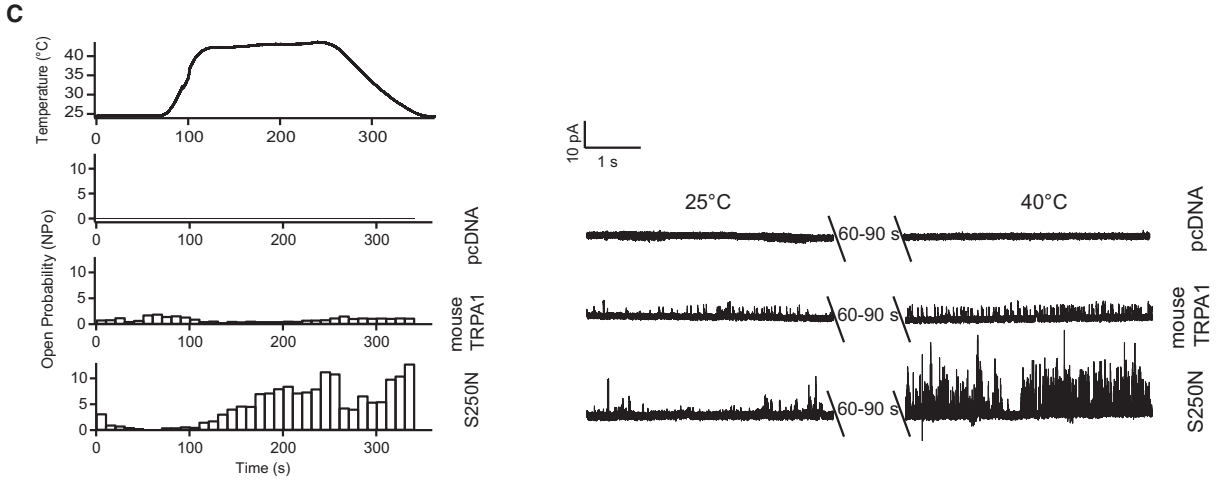

(legend on next page)

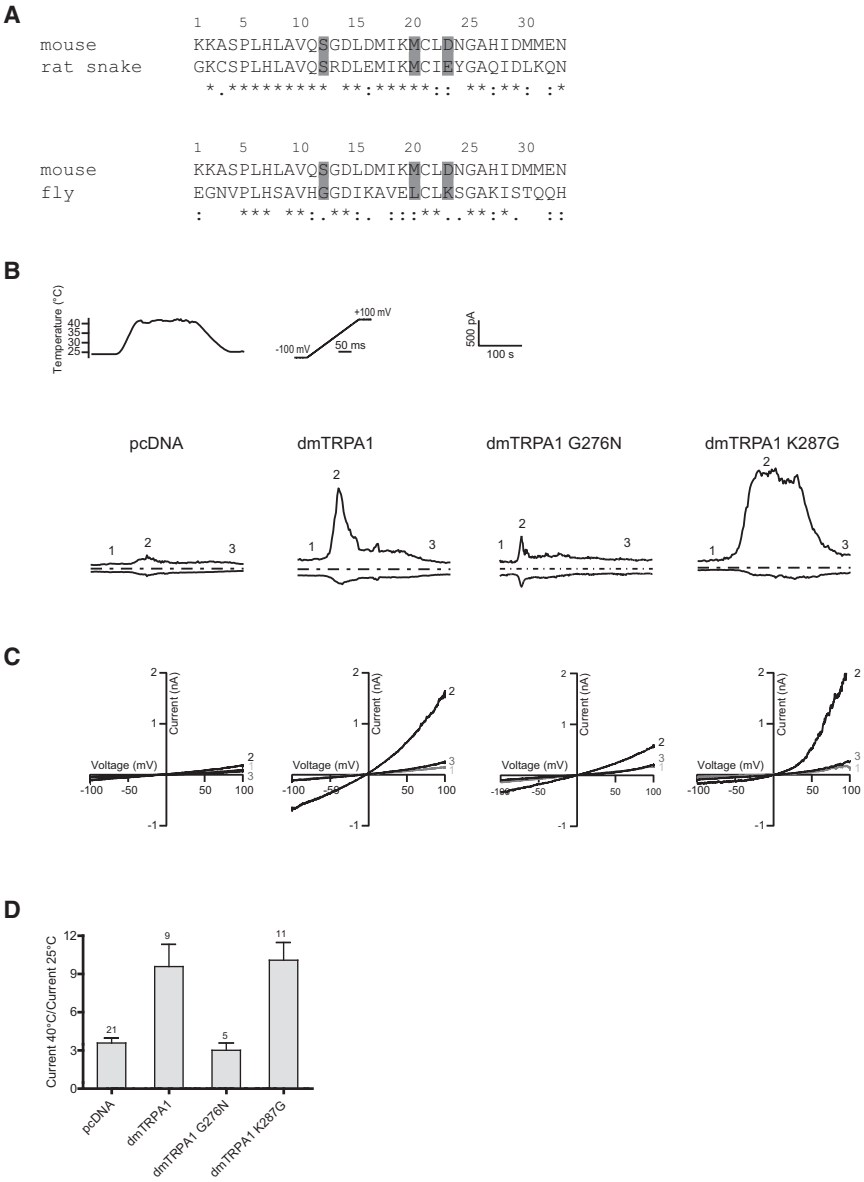

Figure 8. Comparison of Orthologs and Effects on Temperature Sensitivity

(A) Sequence alignments of ankyrin repeat six of wild-type TRPA1 from mouse (*Mus musculus*), rat snake (*Pantherophis obsoletus lindheimeri*), and fruit fly (*Drosophila melanogaster*) generated with ClustalW. "*" indicates identical amino acids and ":" and "." similar amino acids. Residues aligning with identified point mutations are highlighted.

(B) Representative currents evoked by ramp protocol (±100 mV) for pcDNA, wild-type *Drosophila* TRPA1, and *Drosophila* mutants G276N and K287G during a temperature step. Numbers indicate basal currents (1), peak responses (2), and recovery currents (3). Dashed lines represent zero current.

(C) Current-voltage relationships at indicated time points.

(D) Average of maximal current amplitudes at +100 mV. Numbers of experiments are indicated above bars. Data represent mean ± SE.

agarose beads (Pierce) at 4°C with constant rotation for 3 hr or overnight. Biotintylated protein was eluted from beads by heating to 37°C in sample buffer containing 50 mM DTT, and resulting eluent was examined by immunoblot for the myc epitope.

Immunocytochemistry

CHO cells were plated on poly-D-lysine-coated glass bottom dishes (MatTek), additionally coated with laminin (10 μg/ml). Cells were washed three times in prewarmed Hank's balanced salt solution (HBSS) and incubated with wheat germ agglutinin Alexa Fluor 555 conjugate (WGA; 1:100, Invitrogen) diluted in HBSS for 10 min at 37°C. Cells were washed twice in HBSS, once in PBS, and fixed with 4% PFA (paraformaldehyde in PBS). Fixed cells were permeabilized in PBS containing 0.4% Triton X-100, blocked with 10% normal goat serum (NGS in PBS), and incubated for 1 hr in presence of c-*myc* mouse monoclonal antibody (1:1,000 in 1% NGS, Invitrogen). After three washes in PBS, secondary antibody Alexa Fluor 633 goat-anti-mouse IgG (1:500 in 1% NGS, Invitrogen) was added for 1 hr.

Cells were imaged at a Zeiss 780 Axio Observer Z1 microscope (Carl Zeiss MicroImaging) using a 63×/1.4 Oil NA Plan-Apochromat DIC objective, alkali PMT and GaAsP detectors, and Zen 2011 software. Images were taken using identical acquisition parameters. For each experimental group, at least ten TRPA1-positive cells were randomly analyzed. Raw images were analyzed using ImageJ software (NIH). The mean fluorescence intensity of each cell was measured from a 4-pixel-wide band region of interest drawn along the surface of the plasma membrane, as indicated by WGA membrane staining.

Electrophysiology

Patch-clamp recordings were performed using an EPC10 amplifier (HEKA) and Patchmaster software (HEKA). Data were sampled at 20 kHz for single-channel recordings and at 5 kHz for whole-cell recordings and filtered at 2.9 kHz. Borosilicate glass pipettes (Sutter Instruments) had a resistance of 3–6 MΩ

Figure 7. Single-Channel Recordings of Wild-Type Mouse TRPA1 and Mutant S250N

(A) Representative traces of single-channel activity and calculated amplitude histograms in cell-attached patches (+100 mV) at different temperatures. Upward deflections are channel openings. Lines in amplitude histograms indicate fits of two Gaussian functions to the data.

(B) Unitary conductance of wild-type mouse TRPA1 and mutant S250N as a function of temperature. Data represent mean ± SD. Data are averages of five to eight cells and two to five measurements per step protocol. Straight lines indicate exponential fits to the data.

(C) Representative single-channel traces recorded from inside-out patches (+100 mV) at 25°C and 40°C (n = 4 for wild-type mouse TRPA1, pcDNA, and mutant S250N). Recordings were idealized with QuB software and NP_0 calculated (Qin et al., 1996, 1997). Changes in open probability were calculated by averaging NP_o for 60 s at 25°C and 120 s at 40°C.

when filled with pipette buffer solution. Ca^{2+}-free bath solution contained 150 mM NaCl, 1 mM $MgCl_2$, 10 mM glucose, 1 mM EGTA, and 10 mM HEPES (pH 7.4 with NaOH) and the pipette solution 150 mM CsCl, 1 mM $MgCl_2$, 10 mM BAPTA (1, 2-bis [*o*-aminophenoxy] ethane-*N*, *N*, *N*', *N*'- tetraacetic acid), and 10 mM HEPES (pH 7.2 with CsOH). Extracellular solution for Ca^{2+} experiments contained 140 mM NaCl, 5 mM KCl, 2 mM $MgCl_2$, 2 mM $CaCl_2$, 10 mM glucose, and 10 mM HEPES (pH 7.4 with NaOH) and the pipette solution 140 mM KCl, 5 mM EGTA, and 10 mM HEPES (pH 7.4 with KOH). Single-channel recordings were made in the inside-out or the cell-attached configuration. In inside-out recordings, both the pipette solution and the bath solution contained 140 mM NaCl, 5 mM EGTA, and 10 mM HEPES (pH 7.4 with NaOH). Cell-attached recordings were performed in bath solution containing 120 mM KCl, 1 $MgCl_2$, 2 $CaCl_2$, and 5 HEPES (pH 7.4 with KOH) and the pipette solution contained 100 mM KCl, 1 mM $MgCl_2$, 10 mM EGTA, and 10 mM HEPES (pH 7.2 with KOH). Solutions were applied via a gravity-driven perfusion system and the temperature of the solution was controlled by a CL-100 temperature controller (Warner Instruments) and a SC-20 dual in-line heater/cooler (Harvard Apparatus). Temperatures were measured using a TA-29 thermistor (Warner Instruments) placed in line and adjacent to the cell of interest. Experiments probing cold activation of wild-type mouse TRPA1 were done with a custom-built rapid temperature-switching system. The setup consists of two parallel aligned glass pipettes, each perfused by prechilled buffer reservoirs (25°C and 13°C), that could be rapidly positioned to perfuse the measured cell. This setup allowed temperature changes from 25°C to 13°C in less than 10 s. Voltage-step data were derived from cells that demonstrated initial and reversible (after temperature application) >500 MΩ resistance. Voltage-ramp data were obtained from cells with initial resistance of >500 MΩ and at least 50% reduction in heat-induced currents upon reversal to 25°C. For voltage-step protocols, temperature was held constant for ~30 s while voltage-step protocols were executed and then temperature was rapidly changed to the next 5°C increment. Conductance-voltage (G-V) curves were obtained from plateau currents and fitted with a Boltzmann equation to obtain the V_{half}. Temperature dependence of the channel currents was determined by calculating the Q_{10} values according to $Q_{10} = (I_1/I_2)^{10/(T_2-T_1)}$, where I_1 and I_2 are the respective currents at temperatures T_1 and T_2. Activation and deactivation time constants were determined by fitting of exponential functions. To determine the unitary conductance, we calculated amplitude histograms from single-channel recordings at various voltages (+20 to +120 mV). Histograms were fitted with two Gaussian functions. The current difference between both Gaussians was calculated to obtain the single-channel current and the larger of both SDs was used as an error. Calculations were made from five to eight cells and two to five measurements for each voltage step.

Statistical Analysis

Data were analyzed with Igor pro 6.22A (Wavemetrics), Excel (Microsoft), and GraphPad 5.0 prism (GraphPad Software) softwares. Data were tested for statistical significance using an unpaired Student's t test.

SUPPLEMENTAL INFORMATION

Supplemental Information includes one figure and can be found with this article online at http://dx.doi.org/10.1016/j.neuron.2014.04.016.

AUTHOR CONTRIBUTIONS

S.J., R.G., and J.G. designed the study, engineered mutant clones, collected and analyzed data, and wrote the manuscript. J.O.S.-P. collected electrophysiological data. B.K. engineered chimeras. J.W. performed protein stability and localization experiments. J.G. and H.M. performed the mutant library screen and analyzed data. M.B. measured chemical dose-response curves. R.L. and A.P. edited the manuscript.

ACKNOWLEDGMENTS

We thank Manuela Schmidt for advice on immunocytochemistry, Paul Garrity for fly cDNA, and Geoff Pitt for critical reading of the manuscript.

Accepted: March 26, 2014
Published: May 8, 2014

REFERENCES

Baez-Nieto, D., Castillo, J.P., Dragicevic, C., Alvarez, O., and Latorre, R. (2011). Thermo-TRP channels: biophysics of polymodal receptors. Adv. Exp. Med. Biol. *704*, 469–490.

Bandell, M., Dubin, A.E., Petrus, M.J., Orth, A., Mathur, J., Hwang, S.W., and Patapoutian, A. (2006). High-throughput random mutagenesis screen reveals TRPM8 residues specifically required for activation by menthol. Nat. Neurosci. *9*, 493–500.

Banke, T.G., Chaplan, S.R., and Wickenden, A.D. (2010). Dynamic changes in the TRPA1 selectivity filter lead to progressive but reversible pore dilation. Am. J. Physiol. Cell Physiol. *298*, C1457–C1468.

Bobkov, Y.V., Corey, E.A., and Ache, B.W. (2011). The pore properties of human nociceptor channel TRPA1 evaluated in single channel recordings. Biochim. Biophys. Acta *1808*, 1120–1128.

Brauchi, S., Orio, P., and Latorre, R. (2004). Clues to understanding cold sensation: thermodynamics and electrophysiological analysis of the cold receptor TRPM8. Proc. Natl. Acad. Sci. USA *101*, 15494–15499.

Brauchi, S., Orta, G., Salazar, M., Rosenmann, E., and Latorre, R. (2006). A hot-sensing cold receptor: C-terminal domain determines thermosensation in transient receptor potential channels. J. Neurosci. *26*, 4835–4840.

Cao, E., Cordero-Morales, J.F., Liu, B., Qin, F., and Julius, D. (2013). TRPV1 channels are intrinsically heat sensitive and negatively regulated by phosphoinositide lipids. Neuron *77*, 667–679.

Chatzigeorgiou, M., Yoo, S., Watson, J.D., Lee, W.H., Spencer, W.C., Kindt, K.S., Hwang, S.W., Miller, D.M., 3rd, Treinin, M., Driscoll, M., and Schafer, W.R. (2010). Specific roles for DEG/ENaC and TRP channels in touch and thermosensation in C. elegans nociceptors. Nat. Neurosci. *13*, 861–868.

Chen, J., Kim, D., Bianchi, B.R., Cavanaugh, E.J., Faltynek, C.R., Kym, P.R., and Reilly, R.M. (2009). Pore dilation occurs in TRPA1 but not in TRPM8 channels. Mol. Pain *5*, 3.

Chen, J., Kang, D., Xu, J., Lake, M., Hogan, J.O., Sun, C., Walter, K., Yao, B., and Kim, D. (2013). Species differences and molecular determinant of TRPA1 cold sensitivity. Nat Commun *4*, 2501.

Chung, M.K., Güler, A.D., and Caterina, M.J. (2005). Biphasic currents evoked by chemical or thermal activation of the heat-gated ion channel, TRPV3. J. Biol. Chem. *280*, 15928–15941.

Chung, M.K., Güler, A.D., and Caterina, M.J. (2008). TRPV1 shows dynamic ionic selectivity during agonist stimulation. Nat. Neurosci. *11*, 555–564.

Clapham, D.E., and Miller, C. (2011). A thermodynamic framework for understanding temperature sensing by transient receptor potential (TRP) channels. Proc. Natl. Acad. Sci. USA *108*, 19492–19497.

Cordero-Morales, J.F., Gracheva, E.O., and Julius, D. (2011). Cytoplasmic ankyrin repeats of transient receptor potential A1 (TRPA1) dictate sensitivity to thermal and chemical stimuli. Proc. Natl. Acad. Sci. USA *108*, E1184–E1191.

Dhaka, A., Viswanath, V., and Patapoutian, A. (2006). Trp ion channels and temperature sensation. Annu. Rev. Neurosci. *29*, 135–161.

Doerner, J.F., Gisselmann, G., Hatt, H., and Wetzel, C.H. (2007). Transient receptor potential channel A1 is directly gated by calcium ions. J. Biol. Chem. *282*, 13180–13189.

Gaudet, R. (2008). A primer on ankyrin repeat function in TRP channels and beyond. Mol. Biosyst. *4*, 372–379.

Gracheva, E.O., Ingolia, N.T., Kelly, Y.M., Cordero-Morales, J.F., Hollopeter, G., Chesler, A.T., Sánchez, E.E., Perez, J.C., Weissman, J.S., and Julius, D. (2010). Molecular basis of infrared detection by snakes. Nature *464*, 1006–1011.

Grandl, J., Hu, H., Bandell, M., Bursulaya, B., Schmidt, M., Petrus, M., and Patapoutian, A. (2008). Pore region of TRPV3 ion channel is specifically required for heat activation. Nat. Neurosci. *11*, 1007–1013.

Grandl, J., Kim, S.E., Uzzell, V., Bursulaya, B., Petrus, M., Bandell, M., and Patapoutian, A. (2010). Temperature-induced opening of TRPV1 ion channel is stabilized by the pore domain. Nat. Neurosci. *13*, 708–714.

Hinman, A., Chuang, H.H., Bautista, D.M., and Julius, D. (2006). TRP channel activation by reversible covalent modification. Proc. Natl. Acad. Sci. USA *103*, 19564–19568.

Hu, H., Grandl, J., Bandell, M., Petrus, M., and Patapoutian, A. (2009). Two amino acid residues determine 2-APB sensitivity of the ion channels TRPV3 and TRPV4. Proc. Natl. Acad. Sci. USA *106*, 1626–1631.

Jara-Oseguera, A., and Islas, L.D. (2013). The role of allosteric coupling on thermal activation of thermo-TRP channels. Biophys. J. *104*, 2160–2169.

Jordt, S.E., and Julius, D. (2002). Molecular basis for species-specific sensitivity to "hot" chili peppers. Cell *108*, 421–430.

Jordt, S.E., Tominaga, M., and Julius, D. (2000). Acid potentiation of the capsaicin receptor determined by a key extracellular site. Proc. Natl. Acad. Sci. USA *97*, 8134–8139.

Kang, K., Panzano, V.C., Chang, E.C., Ni, L., Dainis, A.M., Jenkins, A.M., Regna, K., Muskavitch, M.A., and Garrity, P.A. (2012). Modulation of TRPA1 thermal sensitivity enables sensory discrimination in Drosophila. Nature *481*, 76–80.

Karashima, Y., Damann, N., Prenen, J., Talavera, K., Segal, A., Voets, T., and Nilius, B. (2007). Bimodal action of menthol on the transient receptor potential channel TRPA1. J. Neurosci. *27*, 9874–9884.

Karashima, Y., Talavera, K., Everaerts, W., Janssens, A., Kwan, K.Y., Vennekens, R., Nilius, B., and Voets, T. (2009). TRPA1 acts as a cold sensor in vitro and in vivo. Proc. Natl. Acad. Sci. USA *106*, 1273–1278.

Kim, S.E., Patapoutian, A., and Grandl, J. (2013). Single residues in the outer pore of TRPV1 and TRPV3 have temperature-dependent conformations. PLoS ONE *8*, e59593.

Latorre, R., Brauchi, S., Orta, G., Zaelzer, C., and Vargas, G. (2007). ThermoTRP channels as modular proteins with allosteric gating. Cell Calcium *42*, 427–438.

Lee, Y., Lee, Y., Lee, J., Bang, S., Hyun, S., Kang, J., Hong, S.T., Bae, E., Kaang, B.K., and Kim, J. (2005). Pyrexia is a new thermal transient receptor potential channel endowing tolerance to high temperatures in Drosophila melanogaster. Nat. Genet. *37*, 305–310.

Liao, M., Cao, E., Julius, D., and Cheng, Y. (2013). Structure of the TRPV1 ion channel determined by electron cryo-microscopy. Nature *504*, 107–112.

Liu, B., Hui, K., and Qin, F. (2003). Thermodynamics of heat activation of single capsaicin ion channels VR1. Biophys. J. *85*, 2988–3006.

Macpherson, L.J., Dubin, A.E., Evans, M.J., Marr, F., Schultz, P.G., Cravatt, B.F., and Patapoutian, A. (2007). Noxious compounds activate TRPA1 ion channels through covalent modification of cysteines. Nature *445*, 541–545.

Matta, J.A., and Ahern, G.P. (2007). Voltage is a partial activator of thermosensitive TRP channels. J. Physiol. *585*, 469–482.

Michaely, P., Tomchick, D.R., Machius, M., and Anderson, R.G. (2002). Crystal structure of a 12 ANK repeat stack from human ankyrinR. EMBO J. *21*, 6387–6396.

Mosavi, L.K., Minor, D.L., Jr., and Peng, Z.Y. (2002). Consensus-derived structural determinants of the ankyrin repeat motif. Proc. Natl. Acad. Sci. USA *99*, 16029–16034.

Mosavi, L.K., Cammett, T.J., Desrosiers, D.C., and Peng, Z.Y. (2004). The ankyrin repeat as molecular architecture for protein recognition. Protein Sci. *13*, 1435–1448.

Nagatomo, K., and Kubo, Y. (2008). Caffeine activates mouse TRPA1 channels but suppresses human TRPA1 channels. Proc. Natl. Acad. Sci. USA *105*, 17373–17378.

Nagatomo, K., Ishii, H., Yamamoto, T., Nakajo, K., and Kubo, Y. (2010). The Met268Pro mutation of mouse TRPA1 changes the effect of caffeine from activation to suppression. Biophys. J. *99*, 3609–3618.

Qin, F., Auerbach, A., and Sachs, F. (1996). Estimating single-channel kinetic parameters from idealized patch-clamp data containing missed events. Biophys. J. *70*, 264–280.

Qin, F., Auerbach, A., and Sachs, F. (1997). Maximum likelihood estimation of aggregated Markov processes. Proc. Biol. Sci. *264*, 375–383.

Salazar, H., Jara-Oseguera, A., Hernández-García, E., Llorente, I., Arias-Olguín, I.I., Soriano-García, M., Islas, L.D., and Rosenbaum, T. (2009). Structural determinants of gating in the TRPV1 channel. Nat. Struct. Mol. Biol. *16*, 704–710.

Sawada, Y., Hosokawa, H., Hori, A., Matsumura, K., and Kobayashi, S. (2007). Cold sensitivity of recombinant TRPA1 channels. Brain Res. *1160*, 39–46.

Story, G.M., Peier, A.M., Reeve, A.J., Eid, S.R., Mosbacher, J., Hricik, T.R., Earley, T.J., Hergarden, A.C., Andersson, D.A., Hwang, S.W., et al. (2003). ANKTM1, a TRP-like channel expressed in nociceptive neurons, is activated by cold temperatures. Cell *112*, 819–829.

Tominaga, M., Caterina, M.J., Malmberg, A.B., Rosen, T.A., Gilbert, H., Skinner, K., Raumann, B.E., Basbaum, A.I., and Julius, D. (1998). The cloned capsaicin receptor integrates multiple pain-producing stimuli. Neuron *21*, 531–543.

Tracey, W.D., Jr., Wilson, R.I., Laurent, G., and Benzer, S. (2003). painless, a Drosophila gene essential for nociception. Cell *113*, 261–273.

Viswanath, V., Story, G.M., Peier, A.M., Petrus, M.J., Lee, V.M., Hwang, S.W., Patapoutian, A., and Jegla, T. (2003). Opposite thermosensor in fruitfly and mouse. Nature *423*, 822–823.

Voets, T. (2012). Quantifying and modeling the temperature-dependent gating of TRP channels. Rev. Physiol. Biochem. Pharmacol. *162*, 91–119.

Voets, T., Droogmans, G., Wissenbach, U., Janssens, A., Flockerzi, V., and Nilius, B. (2004). The principle of temperature-dependent gating in cold- and heat-sensitive TRP channels. Nature *430*, 748–754.

Xiao, B., Dubin, A.E., Bursulaya, B., Viswanath, V., Jegla, T.J., and Patapoutian, A. (2008). Identification of transmembrane domain 5 as a critical molecular determinant of menthol sensitivity in mammalian TRPA1 channels. J. Neurosci. *28*, 9640–9651.

Xiao, R., Zhang, B., Dong, Y., Gong, J., Xu, T., Liu, J., and Xu, X.Z. (2013). A genetic program promotes C. elegans longevity at cold temperatures via a thermosensitive TRP channel. Cell *152*, 806–817.

Yao, J., Liu, B., and Qin, F. (2009). Rapid temperature jump by infrared diode laser irradiation for patch-clamp studies. Biophys. J. *96*, 3611–3619.

Yao, J., Liu, B., and Qin, F. (2010). Kinetic and energetic analysis of thermally activated TRPV1 channels. Biophys. J. *99*, 1743–1753.

Yao, J., Liu, B., and Qin, F. (2011). Modular thermal sensors in temperature-gated transient receptor potential (TRP) channels. Proc. Natl. Acad. Sci. USA *108*, 11109–11114.

Zakharian, E., Cao, C., and Rohacs, T. (2010). Gating of transient receptor potential melastatin 8 (TRPM8) channels activated by cold and chemical agonists in planar lipid bilayers. J. Neurosci. *30*, 12526–12534.

Zhong, L., Bellemer, A., Yan, H., Ken, H., Jessica, R., Hwang, R.Y., Pitt, G.S., and Tracey, W.D. (2012). Thermosensory and nonthermosensory isoforms of Drosophila melanogaster TRPA1 reveal heat-sensor domains of a thermoTRP Channel. Cell Rep *1*, 43–55.

Zurborg, S., Yurgionas, B., Jira, J.A., Caspani, O., and Heppenstall, P.A. (2007). Direct activation of the ion channel TRPA1 by Ca2+. Nat. Neurosci. *10*, 277–279.